

## Near-field imaging of atom diffraction gratings: The atomic Talbot effect

Michael S. Chapman,<sup>1</sup> Christopher R. Ekstrom,<sup>1,\*</sup> Troy D. Hammond,<sup>1</sup> Jörg Schmiedmayer,<sup>1,2</sup> Bridget E. Tannian,<sup>1</sup> Stefan Wehinger,<sup>2</sup> and David E. Pritchard<sup>1</sup>

<sup>1</sup>Department of Physics and Research Laboratory of Electronics, Massachusetts Institute of Technology, Cambridge, Massachusetts 02139

<sup>2</sup>Institut für Experimentalphysik, Universität Innsbruck, Innsbruck, Austria

(Received 4 November 1993)

We have demonstrated the Talbot effect, the self-imaging of a periodic structure, with atom waves. We have measured the successive recurrence of these self-images as a function of the distance from the imaged grating. This is a near-field interference effect, which has several possible applications that are discussed.

PACS number(s): 03.75.Be, 07.60.-j, 42.25.Fx, 42.30.-d

Classical wave optics recognizes two limiting cases, the near and the far field. As the field of atom optics evolves, it is natural to expect interesting developments in both regimes. To date, developments in diffractive atom optics have been concentrated in the far-field regime [1], in which the optical element may be regarded as imparting particular momenta to the atom wave, thereby directing it toward a set of final directions. This is usually accomplished by the absorption of pairs of photons or by diffraction from fabricated structures with locally periodic structure [2]. In the far field, the intensity pattern of the beam is characterized by Fraunhofer diffraction in which the curvature of the atom wave fronts can be neglected. In the near field, however, the curvature of the wave fronts must be considered, and in this case the intensity pattern of the beam is characterized by Fresnel diffraction. Of interest in this paper is a remarkable class of near-field phenomena—the self-imaging of a periodic structure known as the Talbot effect.

Self-imaging of a periodic structure illuminated by quasi-monochromatic coherent light is well known in classical optics and has many applications to image processing and synthesis, photolithography, optical testing, and optical metrology [3]. This effect is also well known in the field of electron optics and has many applications to electron microscopy [4]. It was first observed by Talbot in 1836 [5] and later explained by Rayleigh in 1881 [6]. Rayleigh showed that for a periodic grating illuminated by plane waves, identical self-images of the grating are produced downstream at observation distances that are integral multiples of  $L_{\text{Talbot}} = 2d^2/\lambda$ , where  $d$  is the grating period,  $\lambda$  is the wavelength of the incident radiation, and  $L_{\text{Talbot}}$  is known as the Talbot length. Later workers [7–9] showed that identical self-images, laterally shifted by half a period, are also produced at distances midway between those explained by Rayleigh and that other images with smaller periods  $d/n$  ( $n=2,3,4\dots$ ) are produced at intermediate distances.

The basic Talbot effect can be understood by considering the image formed at  $\frac{1}{2}L_{\text{Talbot}}$ , as shown in Fig. 1. For this case, the path-length differences between different openings

in the grating to a point on the observation plane along the optical axis are integer multiples of  $\lambda$ , and hence an image is formed with the same period as the grating but laterally shifted by half a period. The existence of spatial structure with the period of the grating is also expected downstream of the grating because this region contains overlapping waves whose momenta differ by the reciprocal grating vector. Full treatment of the problem, including predictions of the positions and contrast of the subperiod images, requires solving the Fresnel diffraction problem with more formal techniques [3].

Here, we present measurements of the contrast of successive self-images with atom waves using transmission gratings with two different periods, 200 nm and 300 nm [10]. After discussing the apparatus, procedure, and results, we point out the use of Talbot images for checking grating co-

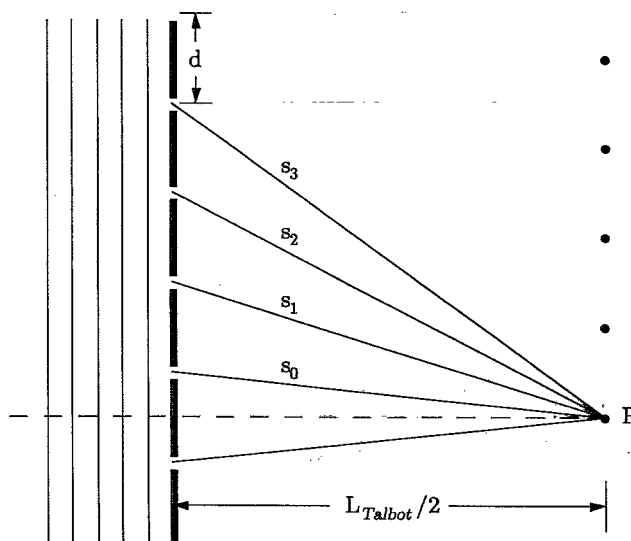


FIG. 1. A simple model illustrating the self-imaging of a grating illuminated by plane waves. It is readily shown that the path lengths  $s_n$  from an opening on the grating to the point  $P$  are given by  $s_n \approx s_0 + n(n+1)\lambda/2$ . Hence, any two path lengths differ by integral multiples of  $\lambda$ , resulting in an intensity maximum at  $P$  and, by symmetry, at the other indicated points.

\*Present address: Department of Physics, University of Konstanz, Germany.

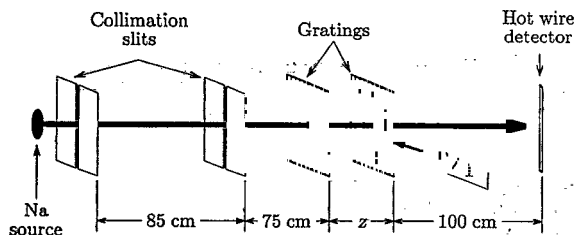


FIG. 2. Schematic of the experimental apparatus. The distance between the two gratings,  $z$ , can be varied from 3.5 to 13.5 mm. The lateral position of the second grating is scanned using the PZT.

herence and suggest a scheme for their use in direct-write atom lithography.

A schematic of the experiment is shown in Fig. 2. Illuminating the first transmission grating by a collimated atom beam produces Talbot self-images of the grating downstream. To detect these images, a second transmission grating is placed downstream to mask the image. If the period of the second grating matches that of the image, it will alternately block and transmit the image as it is laterally scanned, and the total transmitted intensity measured by the detector will display a moiré fringe pattern with respect to the lateral position of the second grating. We measure the contrast of these moiré fringes as a function of the separation between the two gratings. In this experiment, we used gratings of the same period for the first and second gratings and hence expect to see high contrast fringes for grating separations that are half-integral multiples of  $L_{\text{Talbot}}$ .

The atomic-beam system used for this experiment is the same used for our atom-interferometer studies and has been recently described elsewhere [10–12]. We use a well-collimated sodium beam produced by a seeded supersonic source with argon as the carrier gas. Beam collimation is provided by two 20- $\mu\text{m}$  slits separated by 85 cm, yielding a ribbon-shaped beam approximately 20  $\mu\text{m}$  wide by a 0.5 mm high with a beam divergence of 23  $\mu\text{rad}$ . The sodium beam propagates through an evacuated drift region containing two transmission gratings. The transmitted sodium atoms are individually detected by a channel electron multiplier after being ionized by a 50- $\mu\text{m}$  rhenium wire heated to  $\sim 850^\circ\text{C}$ . The background of the detector is typically less than 50 counts/sec. The beam has a mean velocity of  $\sim 1000$  m/sec (corresponding to  $\lambda_{dB} = 0.17 \text{ \AA}$ ) and has an rms velocity width of 3.7%.

The gratings consist of a periodic array of slots etched through a thin ( $\sim 100$  nm) silicon nitride membrane [13]. The gratings are rotationally aligned by maximizing the measured contrast with respect to rotation of the second grating. The second grating is mounted on a translation stage, and the distance between the two gratings,  $z$ , can be varied from 3.5 to 13.5 mm. The point-to-point error associated with each grating translation is less than 10  $\mu\text{m}$ ; however, the absolute grating separation is known only to within 0.5 mm due to the grating mounting system. Grating vibrations are minimized by mechanically isolating the mechanical vacuum pumps in the apparatus, but we made no attempt to measure the residual relative vibrations of the gratings.

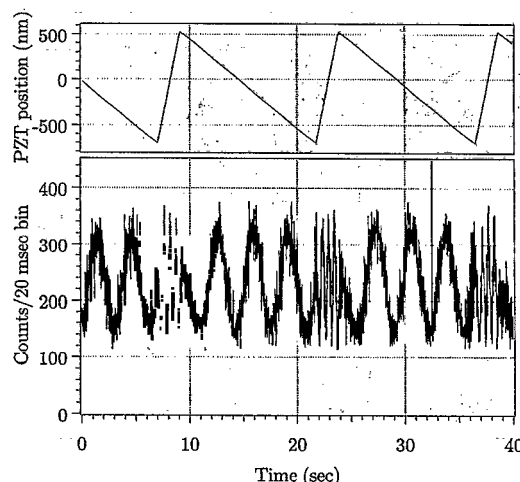


FIG. 3. Detection of the Talbot self-image. The upper graph shows the lateral position of the second grating. The lower graph shows the intensity transmitted through both gratings. A moiré fringe pattern of the intensity is seen as the second grating is scanned across the self-image. The more rapid oscillations come from the fly-back of the PZT. These data were taken with 300-nm gratings separated by  $z \approx \frac{1}{2}L_{\text{Talbot}}$ .

We have performed this experiment with 200- and 300-nm period transmission gratings, which for our atomic beam yield Talbot lengths of 4.7 and 10.6 mm, respectively. The transverse position of the second (mask) grating is scanned using a piezoelectric transducer (PZT) that is calibrated with the laser interferometer described in Ref. [11]. To measure the Talbot image, the total transmitted intensity is recorded as a function of the PZT position. A typical scan is shown in Fig. 3. The distance between the gratings is then varied, and the contrast of the moiré fringe pattern is determined as a function of grating separation.

The experimental results are shown in Fig. 4 for both the 200- and 300-nm gratings. The data demonstrate high-contrast self-images of the first grating at approximate grating separations of  $L_{\text{Talbot}}$  and  $\frac{3}{2}L_{\text{Talbot}}$  for the 200-nm gratings and  $\frac{1}{2}L_{\text{Talbot}}$  for the 300-nm gratings. The contrast of the images damps out for larger grating separations primarily because of the transverse incoherence of the source determined by the collimation of the beam. This effect is illustrated with a simple model in which an extended incoherent source is modeled as an incoherent superposition of point sources [3]. For a grating illuminated by two mutually incoherent point sources laterally separated by  $x$ , it is readily shown that the two self-images produced by these point sources are displaced laterally by  $\Delta x = xz/R$ , where  $R$  is the distance from the point sources to the grating and  $z$  is the distance from the grating to the image plane. Because the two sources are mutually incoherent, the intensities add (not the amplitudes) and the two self-images will wash out when  $\Delta x$  is on the order of half the image period. For our experimental configuration,  $\Delta x \approx 10^{-4}z$ , and hence we would expect the contrast to damp out at  $\sim 10$  mm of grating separation for the 200-nm gratings and at  $\sim 15$  mm for the 300-nm gratings.

In order to compare our results to theory in more detail, we have performed numerical calculations based on a coherent ray-tracing algorithm that was developed to model our

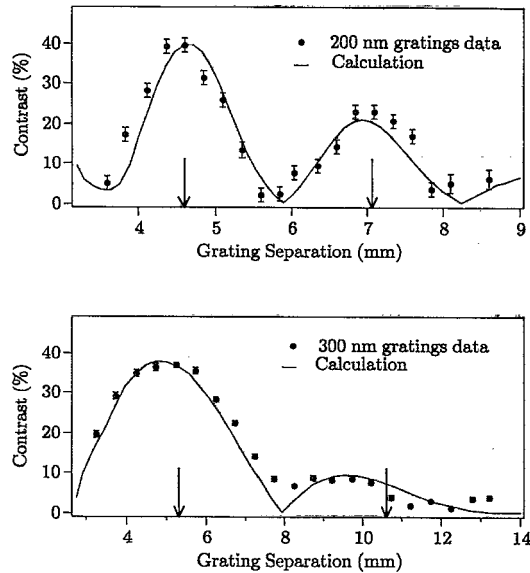


FIG. 4. The experimental data and calculations (see text) showing the contrast of the self-image as a function of grating separation for 200-nm gratings (above) and 300-nm gratings (below). The error bars are statistical only, and positional errors are discussed in the text. The arrows indicate grating separations that are half-integral multiples of  $L_{\text{Talbot}}$ .

atom interferometer [14]. Starting with an extended incoherent polychromatic source, this algorithm performs a coherent sum of the amplitudes for each path through the collimators and gratings. Notably, the calculations do not include effects due to vibrations of the apparatus or grating imperfections such as local variations in grating bar positions or larger-scale phase errors of the gratings. These effects will reduce the contrast of the images and will have a larger effect on the finer period gratings. The maximum measured contrast is  $\sim 60\%$  of the calculated value for the 200-nm gratings and  $\sim 70\%$  of the calculated value for the 300-nm gratings. The calculated contrast as a function of grating separation is compared with our observations in Fig. 4—the curves are normalized to match the measured contrast at the first peak.

Best agreement with the data was obtained by varying two parameters of the calculation—the collimator widths and open fractions of the gratings (defined as the ratio of slot width to grating period). The collimator slits are nominally  $20\ \mu\text{m}$  wide, but can be narrower due to clogging. The best agreement with the data was obtained for a slit width of  $13\ \mu\text{m}$  for the 200-nm data and  $17\ \mu\text{m}$  for the 300-nm data. We attribute this discrepancy to clogging of the collimators, which is consistent with the fact that the collimators were cleaned between the time the 200- and 300-nm data were taken. Effectively narrower collimation slits improve the transverse coherence of the beam and increase the visibility of the contrast revivals as discussed above. The width of the calculated contrast revival peaks depends on the open fractions of the gratings, with larger grating open fractions yielding broader peaks. Best agreement with the 300-nm data was obtained for a 50% open fraction, which agrees well with our estimation of the grating open fraction determined by measuring the relative transmission through the gratings. Similar measurements with the 200-nm gratings indicate an open

fraction of  $\sim 25\%$ , which is somewhat smaller than the 40% open fraction used in the calculation to obtain the best fit. The greater open fraction required to fit the 200-nm data may reflect the greater effect of contrast-lowering imperfections in these finer gratings.

Because of the limitations in the calculations discussed above, a fully quantitative comparison of our experimental results with our calculations is not warranted. However, with reasonable variations of the experimental parameters, we have obtained good agreement with the widths and relative amplitudes of the successive grating images that we observed.

The measurement of the contrast of the self-images sets a limit to the extent of grating imperfections, such as variations in the open fractions and large-scale phase errors, and therefore provides an experimental test of overall grating quality. Indeed, an ancillary motivation for this experimental work was to test the spatial coherence of the gratings we use in our atom interferometer.

As Lau showed in 1948 [15], the requirements on good source collimation to preserve the contrast of the Talbot self-images can be circumvented by using an additional grating placed in front of an extended source. In the Lau effect, which is closely related to the Talbot effect, an additional grating is placed in front of an extended incoherent source, and for particular grating separations, self-images of the second grating are formed. Clauser and Li [16] have recently reported the observation of Lau images in a three-grating atom interferometer [3,11]. Whereas they report the observation of a superposition of reduced period images for a single set of grating separations, we have measured the recurrent self-images of a single grating for a range of observation distances.

A promising application of Talbot (or Lau) imaging with atoms is in the emerging field of atomic lithography [17]. Recent efforts in this field have used resonant light forces. Obviously, fabricated gratings like the ones used here are species unspecific and should work with a variety of materials. This has the additional advantage that the period of the structures produced does not depend on the wavelength of the light resonant with that species. In addition, it should be possible to write smaller features using the reduced period intermediate images discussed above. These images have been used successfully in x-ray lithography to write half-period gratings [18]. It may be possible to use atom beams for this process to write an image directly with the desired material (e.g., silver), which could be subsequently enhanced by electroplating or photographic development. Grating self-images may also be used in quantum-optics experiments to produce a periodic atom density in an optical resonator [19].

In conclusion, we have demonstrated the Talbot effect with atom waves. This is a completely diffractive phenomenon that occurs in the Fresnel diffraction region. We have demonstrated the recurrence of the self-images as a function of the distance from the imaged grating and shown that the results are qualitatively consistent with theoretical predictions.

We acknowledge the technical contributions of Richard Rubenstein. We also thank Michael Rooks and other staff members at the National Nanofabrication Facility. This work

was supported by the U.S. Army Research Office Contracts No. DAAL03-89-K-0082 and No. ASSERT 29970-PH-AAS, the Office of Naval Research Contract No. N00014-89-J-1207, and the Joint Services Electronics Program Contract

No. DAAL03-89-C-0001. T.D.H. acknowledges support from the National Science Foundation. J.S. and S.W. acknowledge support from the University of Innsbruck, Austria.

- 
- [1] Two notable exceptions are near-field atomic diffraction from a slit by J. A. Leavitt and F. A. Bills, *Am. J. Phys.* **37**, 905 (1969); and focusing of an atomic beam with a Fresnel zone plate by O. Carnal, M. Sigel, T. Sleator, H. Takuma, and J. Mlynek, *Phys. Rev. Lett.* **67**, 3231 (1991).
- [2] See, for example, I. Estermann and O. Stern, *Z. Phys.* **37**, 905 (1930); P. L. Gould, G. A. Ruff, and D. E. Pritchard, *Phys. Rev. Lett.* **56**, 827 (1986); D. W. Keith, M. L. Schattenburg, H. I. Smith, and D. E. Pritchard, *ibid.* **61**, 1580 (1988); M. Kasevich and S. Chu, *ibid.* **67**, 181 (1991); O. Carnal, A. Faulstich, and J. Mlynek, *Appl. Phys. B* **53**, 88 (1991).
- [3] See the recent review by K. Paturski, in *Progress in Optics*, edited by E. Wolf (North-Holland, Amsterdam, 1989), Vol. 27.
- [4] R. D. Heidenrich, *Fundamentals of Transmission Electron Microscopy* (Interscience, New York, 1964).
- [5] H. F. Talbot, *Philos. Mag.* **9**, 401 (1836).
- [6] L. Rayleigh, *Philos. Mag.* **11**, 196 (1881).
- [7] J. Cowley and A. Moodie, *Proc. Phys. Soc. B* **70**, 486 (1957); **70**, 497 (1957); **70**, 505 (1957).
- [8] G. L. Rogers, *Br. J. Appl. Phys.* **15**, 594 (1964).
- [9] J. T. Winthrop and C. R. Worthington, *J. Opt. Soc. Am.* **55**, 373 (1965).
- [10] J. Schmiedmayer, C. R. Ekstrom, M. S. Chapman, T. D. Hammond, and D. E. Pritchard, in *Fundamentals of Quantum Optics III*, Proceedings, Kühtai, Austria, edited by F. Ehlotzky, Lecture Notes in Physics Vol. 420 (Springer-Verlag, Berlin, 1993). In this paper, we reported the observation of Talbot images for atoms at a single-grating separation.
- [11] D. W. Keith, C. R. Ekstrom, Q. A. Turchette, and D. E. Pritchard, *Phys. Rev. Lett.* **66**, 2693 (1991).
- [12] C. R. Ekstrom, Ph.D. thesis, Massachusetts Institute of Technology, 1993 (unpublished).
- [13] C. R. Ekstrom, D. W. Keith, and D. W. Pritchard, *Appl. Phys. B* **54**, 369 (1992).
- [14] Q. A. Turchette, D. E. Pritchard, and D. W. Keith, *J. Opt. Soc. Am. B* **9**, 1601 (1992).
- [15] E. Lau, *Ann. Phys. (Leipzig)* **6**, 417 (1948).
- [16] J. F. Clauser and S. Li, *Phys. Rev. A* **49**, R2213 (1994).
- [17] G. Timp, R. E. Behringer, D. M. Tennant, J. E. Cunningham, M. Prentiss, and K. K. Berggren, *Phys. Rev. Lett.* **69**, 1636 (1992); J. J. McClelland, R. E. Scholten, E. C. Palm, and R. J. Celotta, *Science* **262**, 877 (1993).
- [18] D. C. Flanders, A. M. Hawryluk, and H. I. Smith, *J. Vac. Sci. Technol.* **16**, 1949 (1979).
- [19] O. Carnal, Q. A. Turchette, and H. J. Kimble (unpublished).